Acta Crystallographica Section F
Structural Biology and Crystallization Communications
ISSN 1744-3091

Crystallization and preliminary X-ray diffraction analysis of motif N from *Saccharomyces cerevisiae* Dbf4

Lindsay A. Matthews,[a] Andrew Duong,[a] Ajai A. Prasad,[b] Bernard P. Duncker[b] and Alba Guarné[a]*

[a]Department of Biochemistry and Biomedical Sciences, HSC-4N57A, McMaster University, Hamilton, ON L8N 3Z5, Canada, and [b]Department of Biology, University of Waterloo, Waterloo, ON N2L 3G1, Canada

Correspondence e-mail: guarnea@mcmaster.ca

Received 24 April 2009
Accepted 23 July 2009

The Cdc7–Dbf4 complex plays an instrumental role in the initiation of DNA replication and is a target of replication-checkpoint responses in *Saccharomyces cerevisiae*. Cdc7 is a conserved serine/threonine kinase whose activity depends on association with its regulatory subunit, Dbf4. A conserved sequence near the N-terminus of Dbf4 (motif N) is necessary for the interaction of Cdc7–Dbf4 with the checkpoint kinase Rad53. To understand the role of the Cdc7–Dbf4 complex in checkpoint responses, a fragment of *Saccharomyces cerevisiae* Dbf4 encompassing motif N was isolated, overproduced and crystallized. A complete native data set was collected at 100 K from crystals that diffracted X-rays to 2.75 Å resolution and structure determination is currently under way.

1. Introduction

The initiation of DNA replication requires the formation of a pre-replicative complex at the origins and the activity of two kinases, which are known as Cdc28 and Cdc7 in the budding yeast *Saccharomyces cerevisiae* (Bell & Dutta, 2002). In this organism, the activity of Cdc28 is regulated by six different cyclins, while that of Cdc7 depends on a single regulatory subunit, the Dbf4 protein (Diffley, 1998; Jackson *et al.*, 1993; Ogino *et al.*, 2001). The Cdc7–Dbf4 complex, also known as DDK (Dbf4-dependent kinase), phosphorylates targets found at licensed origins, triggering the onset of DNA replication, and plays an integral role during cellular checkpoint responses (Masai & Arai, 2002; Sclafani, 2000). During genotoxic stress, the Cdc7–Dbf4 complex is thought to phosphorylate the checkpoint kinase Rad53, leading to its full activation (Ogi *et al.*, 2008). Dbf4 is then phosphorylated in a Rad53-dependent manner, causing its dissociation from chromatin and the inhibition of Cdc7 kinase activity (Kihara *et al.*, 2000; Weinreich & Stillman, 1999), consequently regulating DNA replication by suppressing the activation of unfired origins (Bousset & Diffley, 1998; Donaldson *et al.*, 1998; Pasero *et al.*, 1999).

Dbf4 orthologues are variable in length and sequence but encompass three conserved motifs named N, M and C based on their relative location in the polypeptide chain (Masai & Arai, 2000). In *S. cerevisiae*, motifs M (residues 260–309) and C (residues 659–696) are included within regions that have been shown to interact with Cdc7 (Dowell *et al.*, 1994; Hardy & Pautz, 1996). Additionally, motif M mediates the association between Dbf4 and the Mcm2 protein, a subunit of the hexameric MCM ring within the pre-replicative complex (Lei *et al.*, 1997; Varrin *et al.*, 2005). Motif N (residues 129–177) mediates interactions with both the Orc2 subunit of the origin-recognition complex (ORC) and the checkpoint kinase Rad53 (Varrin *et al.*, 2005). Based on primary sequence analysis, it has been suggested that residues 117–218, encompassing the entire motif N, could resemble a BRCT domain with a divergent C-terminus (Gabrielse *et al.*, 2006). Originally identified at the C-terminus of the BRCA-1 protein, BRCT domains are widely found in DNA-repair and replication-checkpoint proteins (Bork *et al.*, 1997), reinforcing the idea that Dbf4 could mediate protein–protein interactions during

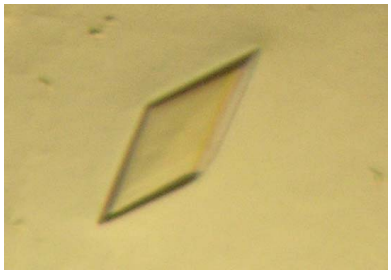

Figure 1
Sequence and secondary-structure prediction of Dbf4 (residues 101–260). The fragments generated for crystallization are indicated by double-headed arrows and labelled. Residues 129–177, originally identified as motif N (Masai & Arai, 2000), are shaded. Predicted secondary-structure elements are shown as cylinders (α-helices) and arrows (β-strands).

checkpoint responses. However, the specific interactions that mediate the association of Cdc7–Dbf4 with Rad53 and the consequent phosphorylation of Rad53 and Dbf4 remain unclear.

In an effort to understand how Dbf4 mediates the interaction between Cdc7–Dbf4 and Rad53, we overproduced, purified and crystallized Dbf4-N (residues 120–250), a segment of *S. cerevisiae* Dbf4 encompassing motif N. Here, we describe the methods used to improve crystal nucleation and growth, as well as the preliminary X-ray analysis of Dbf4-N crystals diffracting to 2.75 Å resolution.

2. Experimental methods

2.1. Cloning and solubility assays

Three constructs encompassing motif N of *S. cerevisiae* Dbf4 were generated: residues 120–250 (pAG8206), residues 120–220 (pAG8207) and residues 105–250 (pAG8208) (Fig. 1). These *DBF4* fragments were subcloned into the pET15b vector (Novagen) using *Nde*I and *Bam*HI restriction sites and confirmed by DNA sequencing (MOBIX Laboratory, McMaster University). The resulting recombinant proteins included a histidine tag (removable by thrombin digestion) at their N-termini. To test solubility, the proteins were overproduced in *Escherichia coli* BL21 Star (DE3) cells (Invitrogen Life Technologies) containing a plasmid encoding tRNA molecules rarely used in *E. coli* (pRARELysS). The cell cultures were grown to an OD_{600} of ~0.7 at 310 K prior to inducing protein production by the addition of 1 m*M* isopropyl β-D-1-thiogalactopyranoside. Cells were harvested by centrifugation after either 3 h at 310 K, 5 h at 298 K or 12 h at 289 K and were lysed using a combination of lysozyme (0.5 mg ml^{-1}), salt (0.5 *M* NaCl) and detergent (0.03% lauryl dimethylamine *N*-oxide). The solubility of each fragment was assessed on 15% SDS polyacrylamide gels stained with Coomassie Brilliant Blue.

2.2. Protein expression and purification

Cells producing Dbf4-N (residues 120–250) were harvested after 5 h at 298 K and washed with phosphate-buffered saline. Cell pellets were resuspended in buffer *A* (20 m*M* Tris pH 8.0, 500 m*M* NaCl, 1.4 m*M* β-mercaptoethanol, 15 m*M* imidazole and 5% glycerol) and lysed by sonication. Cell lysates were subsequently clarified by centrifugation (39 000*g* at 277 K for 40 min). The supernatant was loaded onto a 5 ml HiTrap HP column (GE Healthcare) charged with Ni^{2+}. The column was then washed with buffer *A*, followed by buffer *A* supplemented with 36 m*M* imidazole. Dbf4-N was eluted with 300 m*M* imidazole and further purified by ion exchange on a MonoS 10/100 GL column (GE Healthcare) equilibrated with 20 m*M* Tris pH 8.0, 1 m*M* EDTA, 5 m*M* DTT, 100 m*M* NaCl and 5% glycerol. Pure Dbf4-N was eluted from the column using a linear gradient to 500 m*M* NaCl, concentrated to 7 mg ml^{-1} and stored in 20 m*M* Tris pH 8.0, 100 m*M* NaCl, 1 m*M* DTT and 5% glycerol (Fig. 2*a*). Protein concentration was estimated using a Bradford assay (Bradford, 1976).

2.3. Crystallization and data collection

Crystallization drops were prepared at 277 K by mixing 1 µl protein solution (7 mg ml^{-1}) with 1 µl crystallization solution [27–28% PEG 400, 0.05 *M* $MgCl_2$, 0.1 *M* Tris pH 8.5 and 4–5.5% penta-

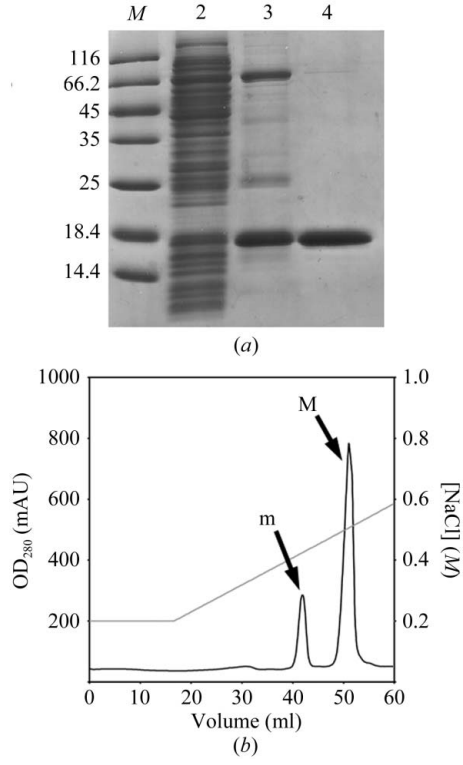

Figure 2
Protein expression and purification of Dbf4 fragments encompassing motif N. (*a*) Coomassie-stained 15% SDS polyacrylamide gel depicting the purification steps of the major isoform of Dbf4-N (120–250). Lane *M*, molecular-weight markers (labelled in kDa); lane 2, cell lysate; lane 3, after elution from Ni-affinity column; lane 4, after elution from MonoS column. (*b*) Chromatogram corresponding to the elution of Dbf4-N (120–250) from a MonoS 10/100 GL column (GE Healthcare). The major (M) and minor (m) isoforms are indicated.

erythritol ethoxylate (PEE)] and subsequently equilibrated against increasing concentrations of ammonium sulfate (0.5–2.5 *M*) using a modified vapour-diffusion protocol as described previously (Dunlop & Hazes, 2005; Newman, 2005). Crystals of Dbf4-N were flash-cooled in liquid nitrogen. A complete data set was collected on the X29 beamline of the National Synchrotron Light Source (NSLS), Brookhaven National Laboratory (BNL) using 1° oscillations and a crystal-to-detector distance of 300 mm. Diffraction data were indexed, integrated and scaled using the *HKL*-2000 package (Otwinowski & Minor, 1997).

3. Results and discussion

3.1. Domain boundaries of motif N

Motif N was originally reported as encompassing residues 129–177 and its resemblance to BRCT domains has been noted (Masai & Arai, 2000). In a subsequent study, the region surrounding motif N (residues 117–218) was predicted to define a BRCT domain with a divergent sequence at its C-terminus that is exclusively found in Dbf4 proteins (Gabrielse *et al.*, 2006). Based on these two reports and secondary-structure predictions of multiple Dbf4 orthologues using *PSIPRED* (Bryson *et al.*, 2005), three different constructs were generated that differed in the structural elements included at the domain boundaries (Fig. 1). While the fragment encompassing residues 120–220 included the predicted BRCT motif of Dbf4, it exhibited minimal expression and solubility levels. The inclusion of an additional fragment at the C-terminus (residues 120–250) increased both the expression and the solubility of the fragment, while the addition of residues 105–119 at the N-terminus was without effect. Therefore, subsequent crystallographic analysis was conducted using the fragment encompassing residues 120–250, which is hereafter referred to as Dbf4-N.

3.2. Crystallization of Dbf4-N

Two different isoforms of Dbf4-N were isolated using cation-exchange chromatography (Fig. 2*b*). Both isoforms behaved as monomers in solution as judged by size-exclusion chromatography (data not shown). However, mass-spectrometric analysis revealed that while the major isoform (17 346 Da) corresponded to unmodified Dbf4-N, the minor isoform was a mixture of two modified species with molecular weights of 17 389 and 17 525 Da. Therefore, only the major isoform was used for subsequent crystallization analysis.

Dbf4-N crystals only appeared after stepwise dehydration with 0.5–2.5 *M* ammonium sulfate for at least two weeks and grew to their maximum size in about two months (Fig. 3). Optimization of the protein or precipitant concentration, the pH, the ionic strength or the type of precipitant did not change the nucleation of Dbf4-N crystals. We entertained the idea that delayed crystallization was a consequence of protein degradation, but mass spectrometry of the crystals revealed that they contained intact Dbf4-N (data not shown). It has previously been shown that ammonium sulfate can trigger pH changes owing to ammonia transfer following ammonium–ammonia

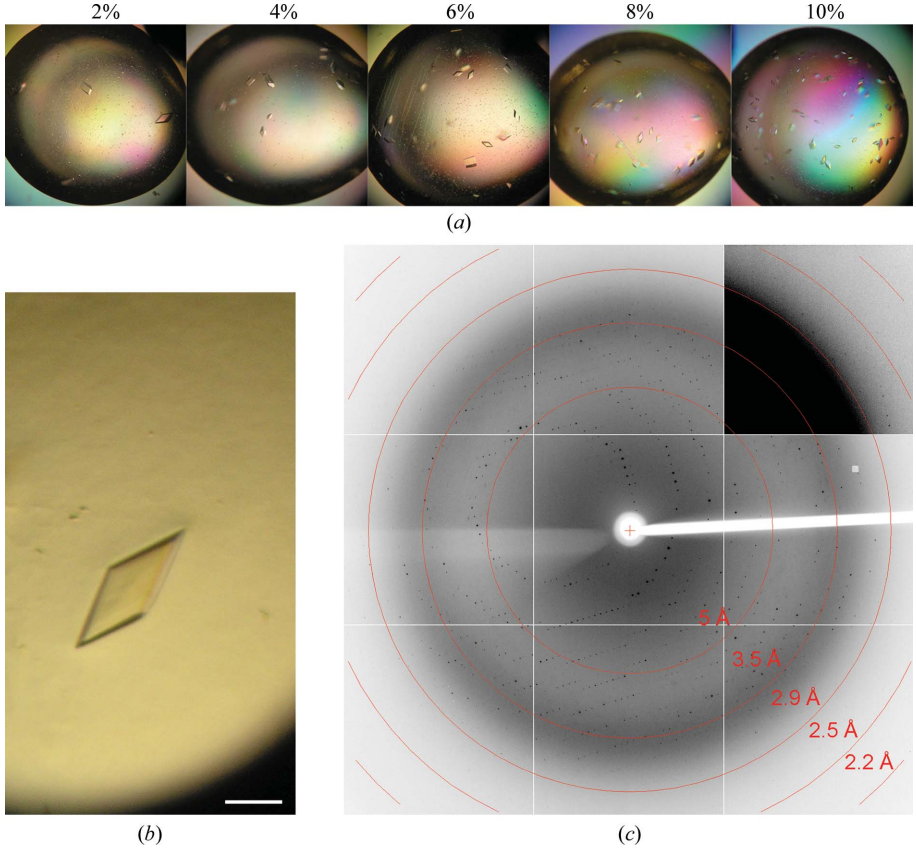

Figure 3
Crystallization and diffraction of Dbf4-N (120–250). (*a*) The effect of pentaerythritol ethoxylate (PEE) on the crystallization of Dbf4-N. Increasing concentrations of PEE favour nucleation but decrease crystal size (left to right). (*b*) Representative crystals of Dbf4-N (120–250) grown in 27.6% PEG 400, 0.05 *M* $MgCl_2$, 0.1 *M* Tris pH 8.5 and 4–5% PEE. The scale bar represents 0.1 mm. (*c*) Representative X-ray diffraction pattern of a Dbf4-N (120–250) crystal collected on beamline X29 (NSLS, BNL). Data were collected at a crystal-to-detector distance of 300 mm and a wavelength of 1.29 Å. The resolution at the detector edge is 2.6 Å. In the top right inset, the darkness of the image has been adjusted to highlight weak reflections.

Table 1
Data-collection statistics for Dbf4-N (120–250) crystals.

Values in parentheses are for the highest resolution shell.

Experimental conditions	
X-ray source	X29 (NSLS, BNL)
Wavelength (Å)	1.29
Temperature (K)	100
Detector	ADSC Q315 CCD
No. of images	100
Exposure time (s)	20
Oscillation angle (°)	1
Data processing	
No. of measured reflections	77857
No. of unique reflections	41469
Space group	$P2_1$
Unit-cell parameters (Å, °)	a = 89.7, b = 79.1, c = 127.3, β = 110.6
Resolution (Å)	25–2.75 (2.85–2.75)
Completeness (%)	95.1 (97.9)
Multiplicity	1.9 (1.8)
Mean $I/\sigma(I)$	14.8 (1.8)
$R_{\rm merge}$	0.057 (0.462)
No. of molecules per ASU	10
Matthews coefficient $V_{\rm M}$ (Å^3 Da^{-1})	2.42
Solvent content (%)	49

equilibrium (Mikol *et al.*, 1989), suggesting that the formation of Dbf4-N crystals was partially driven by a pH gradient.

In order to grow suitable crystals for X-ray diffraction, we screened a battery of crystallization additives. Pentaerythritol ethoxylate (PEE) decreased the solubility of Dbf4-N since crystals started appearing in drops equilibrated against 1.5 *M* rather than 2.5 *M* ammonium sulfate. Although PEE was initially identified as a promising precipitant that increased the quality of crystals (Gulick *et al.*, 2002), in this instance it presumably acted by enhancing crystal nucleation. However, we found that it could only substitute for PEG 400 in limited amounts because the PEE concentration was positively correlated with the number of crystals obtained (Fig. 3*a*). As such, PEE represented a trade-off between decreasing the time required for crystallization and a reduction in crystal size owing to enhanced nucleation. Optimal Dbf4-N crystals were grown in 27–28% PEG 400, 0.05 *M* $MgCl_2$, 0.1 *M* Tris pH 8.5 and 4–5.5% PEE and grew to approximate dimensions of 0.2 × 0.1 × 0.05 mm (Fig. 3*b*).

3.3. Diffraction analysis of Dbf4-N crystals

The Dbf4-N (120–250) crystals belonged to space group $P2_1$, with unit-cell parameters a = 89.7, b = 79.1, c = 127.3 Å, β = 110.6° (Table 1). According to the Matthews coefficient calculation, there could be between eight ($V_{\rm M}$ = 3.02 Å^3 Da^{-1}) and 12 ($V_{\rm M}$ = 2.01 Å^3 Da^{-1}) molecules in the asymmetric unit. Analysis of the self-rotation function calculated with *MOLREP* revealed the presence of perpendicular twofold axes, as well as two pseudo-fivefold axes (κ = 71.75°; Collaborative Computational Project, Number 4, 1994). The quasi-fivefold symmetry supports the presence of ten molecules ($V_{\rm M}$ = 2.42 Å^3 Da^{-1}) in the asymmetric unit over the other possible cell contents (Table 1). Interestingly, it has previously been shown that oligomers of the Cdc7–Dbf4 kinase exist in *S. cerevisiae* and it has been suggested that oligomerization may play a regulatory role (Shellman *et al.*, 1998). However, the nature of these oligomers is still unclear.

We tried to solve the Dbf4-N structure by molecular replacement using various structures containing single BRCT domains (PDB codes 2jw5, 2ebu, 1l7b and 2ebw). Structures containing tandem BRCT repeats were excluded from our list because the interdomain linker is believed to pose restrictions on the overall BRCT fold (Glover *et al.*, 2004) which would not exist in proteins containing a single BRCT domain such as Dbf4. Dbf4-N only has around 10% sequence identity and 30–35% sequence similarity to these BRCT domains; however, these values are similar to those obtained when comparing bona fide BRCT domains using structure-guided sequence alignments.

Unfortunately, none of these models yielded a solution for the structure of Dbf4-N. The lack of successful results using various molecular-replacement protocols could have been caused by several factors. Firstly, BRCT domains are notoriously flexible and flexibility is known to jeopardize structure determination by molecular replacement. However, the results obtained using search models generated as ensembles of multiple structures were similar to those obtained using models containing a single BRCT structure. Secondly, the asymmetric unit of the Dbf4-N crystal presumably includes ten Dbf4-N molecules, creating a disproportionate ratio between the volume of the search model and the volume being searched. Thirdly, Dbf4-N is proposed to fold as a noncanonical BRCT domain with its C-terminus adopting a structure that is unique to the Dbf4 family (Gabrielse *et al.*, 2006). Indeed, the N- and C-terminal ends of the BRCT domains used for molecular replacement are extremely variable, suggesting that the BRCT fold can withstand both flexibility and sequence variability. To overcome these potential problems, structure determination using multiple anomalous diffraction is currently under way.

We thank Ms Yu Seon Chung and the PXRR staff at the NSLS (BNL) for assistance during data collection. LAM was supported by a CIHR scholarship. This work was supported by the Canadian Institutes of Health Research (MOP 67189 to AG) and NSERC (RGPIN 238392 to BPD).

References

Bell, S. P. & Dutta, A. (2002). *Annu. Rev. Biochem.* **71**, 333–374.
Bork, P., Hofmann, K., Bucher, P., Neuwald, A. F., Altschul, S. F. & Koonin, E. V. (1997). *FASEB J.* **11**, 68–76.
Bousset, K. & Diffley, J. F. (1998). *Genes Dev.* **12**, 480–490.
Bradford, M. M. (1976). *Anal. Biochem.* **72**, 248–254.
Bryson, K., McGuffin, L. J., Marsden, R. L., Ward, J. J., Sodhi, J. S. & Jones, D. T. (2005). *Nucleic Acids Res.* **33**, W36–W38.
Collaborative Computational Project, Number 4 (1994). *Acta Cryst.* D**50**, 760–763.
Diffley, J. F. (1998). *Curr. Biol.* **8**, R771–R773.
Donaldson, A. D., Fangman, W. L. & Brewer, B. J. (1998). *Genes Dev.* **12**, 491–501.
Dowell, S. J., Romanowski, P. & Diffley, J. F. (1994). *Science*, **265**, 1243–1246.
Dunlop, K. V. & Hazes, B. (2005). *Acta Cryst.* D**61**, 1041–1048.
Gabrielse, C., Miller, C. T., McConnell, K. H., DeWard, A., Fox, C. A. & Weinreich, M. (2006). *Genetics*, **173**, 541–555.
Glover, J. N., Williams, R. S. & Lee, M. S. (2004). *Trends Biochem. Sci.* **29**, 579–585.
Gulick, A. M., Horswill, A. R., Thoden, J. B., Escalante-Semerena, J. C. & Rayment, I. (2002). *Acta Cryst.* D**58**, 306–309.
Hardy, C. F. & Pautz, A. (1996). *Mol. Cell. Biol.* **16**, 6775–6782.
Jackson, A. L., Pahl, P. M., Harrison, K., Rosamond, J. & Sclafani, R. A. (1993). *Mol. Cell. Biol.* **13**, 2899–2908.
Kihara, M., Nakai, W., Asano, S., Suzuki, A., Kitada, K., Kawasaki, Y., Johnston, L. H. & Sugino, A. (2000). *J. Biol. Chem.* **275**, 35051–35062.
Lei, M., Kawasaki, Y., Young, M. R., Kihara, M., Sugino, A. & Tye, B. K. (1997). *Genes Dev.* **11**, 3365–3374.
Masai, H. & Arai, K. (2000). *Biochem. Biophys. Res. Commun.* **275**, 228–232.
Masai, H. & Arai, K. (2002). *J. Cell. Physiol.* **190**, 287–296.
Mikol, V., Rodeau, J.-L. & Giegé, R. (1989). *J. Appl. Cryst.* **22**, 155–161.
Newman, J. (2005). *Acta Cryst.* D**61**, 490–493.
Ogi, H., Wang, C. Z., Nakai, W., Kawasaki, Y. & Masumoto, H. (2008). *Gene*, **414**, 32–40.

Ogino, K., Takeda, T., Matsui, E., Iiyama, H., Taniyama, C., Arai, K. & Masai, H. (2001). *J. Biol. Chem.* **276**, 31376–31387.
Otwinowski, Z. & Minor, W. (1997). *Methods Enzymol.* **276**, 307–326.
Pasero, P., Duncker, B. P., Schwob, E. & Gasser, S. M. (1999). *Genes Dev.* **13**, 2159–2176.
Sclafani, R. A. (2000). *J. Cell Sci.* **113**, 2111–2117.
Shellman, Y. G., Schauer, I. E., Oshiro, G., Dohrmann, P. & Sclafani, R. A. (1998). *Mol. Gen. Genet.* **259**, 429–436.
Varrin, A. E., Prasad, A. A., Scholz, R. P., Ramer, M. D. & Duncker, B. P. (2005). *Mol. Cell. Biol.* **25**, 7494–7504.
Weinreich, M. & Stillman, B. (1999). *EMBO J.* **18**, 5334–5346.